iScience

Article

Characterization of $G\alpha_s$ and $G\alpha_{olf}$ activation by catechol and non-catechol dopamine D1 receptor agonists

Graphical abstract

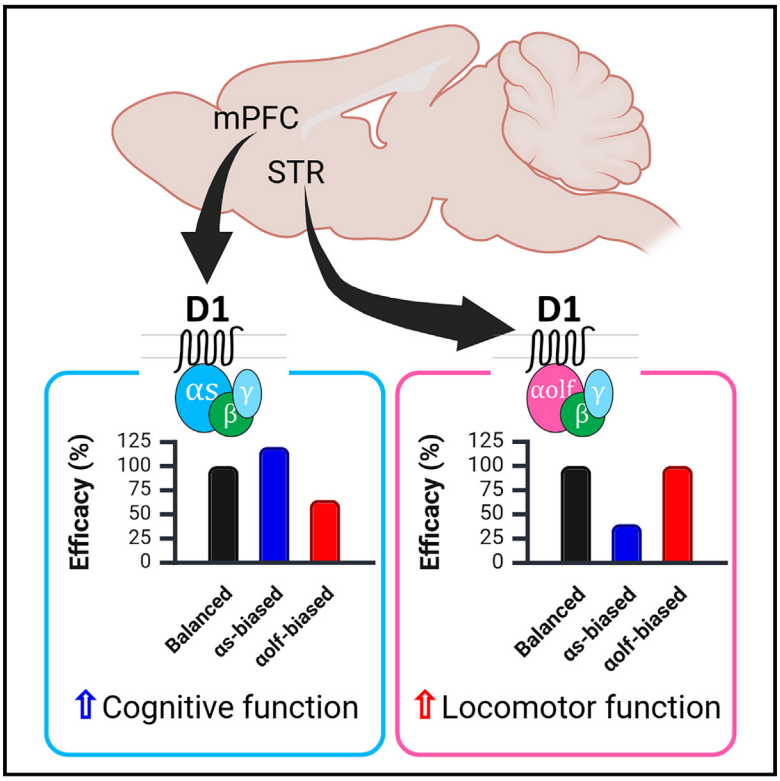

Authors

Anh Minh Nguyen, Ana Semeano, Vianna Quach, Asuka Inoue, David E. Nichols, Hideaki Yano

Correspondence

h.yano@northeastern.edu

In brief

Molecular biology; Neuroscience

Highlights

- Some D1R agonists displayed selective activation profiles toward $G\alpha_s$ or $G\alpha_{olf}$
- The selective *in vitro* profiles translate to their electrophysiological and behavioral effects
- The αN domain of the Gα protein contributes to this subtype selectivity of D1R

Nguyen et al., 2025, iScience *28*, 112345
May 16, 2025
https://doi.org/10.1016/j.isci.2025.112345

CellPress

iScience

CellPress
OPEN ACCESS

Article

Characterization of $G\alpha_s$ and $G\alpha_{olf}$ activation by catechol and non-catechol dopamine D1 receptor agonists

Anh Minh Nguyen,[1] Ana Semeano,[1] Vianna Quach,[1] Asuka Inoue,[2] David E. Nichols,[3] and Hideaki Yano[1,4,*]

[1]Department of Pharmaceutical Sciences, School of Pharmacy and Pharmaceutical Sciences, Bouvé College of Health Sciences, Center for Drug Discovery, Northeastern University, Boston, MA, USA

[2]Graduate School of Pharmaceutical Sciences, Tohoku University, Sendai, Miyagi, Japan

[3]Division of Chemical Biology and Medicinal Chemistry, Eshelman School of Pharmacy, University of North Carolina, Chapel Hill, NC, USA

[4]Lead contact

*Correspondence: h.yano@northeastern.edu

https://doi.org/10.1016/j.isci.2025.112345

SUMMARY

The dopamine D1 receptor (D1R) couples to $G\alpha_s$ and $G\alpha_{olf}$ and is crucial in regulating neurological and neuropsychiatric functions. In the brain, $G\alpha_{olf}$ is predominantly found in the striatum whereas $G\alpha_s$ is expressed elsewhere. Our *in vitro* assays revealed that the tetracyclic catechol agonists dihydrexidine, methyl-dihydrexidine, doxanthrine, and the non-catechol compounds PF-8294, PF-6142 exerted full agonism for $G\alpha_s$ coupling but only partial agonism for $G\alpha_{olf}$ coupling. In contrast, the non-catechol agonist tavapadon acted as a full agonist at $G\alpha_{olf}$ and a partial agonist at $G\alpha_s$. The effects of these ligands on the thalamocortical and striatonigral electrophysiological events, as well as on the locomotor activity and cognitive function of mice agreed with their selectivity profiles *in vitro*. These findings suggest the possibility of achieving region-specific pharmacology and open new directions for developing D1R drugs to treat relevant neurological and neuropsychiatric disorders.

INTRODUCTION

The dopamine D1 receptor (D1R) is one of the most widely expressed dopamine (DA) receptor subtypes in the mammalian central nervous system (CNS)[1] as DA receptors regulate a breadth of important physiological and behavioral functions.[2,3] D1R activation has been reported to stimulate locomotor activity,[4,5] drive motivation and reward-associated behaviors,[6,7] and mediate executive functions and working memory.[8–10] Thus, D1R appears to be a promising target for drug development against several neuropsychiatric disorders, including Parkinson's disease (PD) and schizophrenia.

Developing selective D1R agonists has proven to be challenging. Classic selective D1R agonists usually contain the catechol moiety of DA. Although some D1R agonists exhibited promising effects on cognitive function[11] and locomotor activity,[12] with some even advancing to clinical trials,[13,14] they were prematurely terminated due to their severe side effects, unfavorable pharmacokinetic properties, and tolerance.[14–17] Because of these issues, there is a dire need for new D1R agonists that can overcome these limitations but are equally efficacious. In recent years, a new class of D1R agonists without the catechol moiety has been discovered.[18–21] Remarkably, a few ligands from this class have demonstrated antiparkinsonian effects, encouraging pharmacokinetic profiles, and limited tolerance.[22–27] However, little is known about their pharmacological differences because the conventional catechol and novel non-catechol agonists have not been compared in various assay modalities in a systematic way.

Selectively activating D1Rs in the medial prefrontal cortex (mPFC) and the striatum has been suggested to be beneficial in treating the negative symptoms of schizophrenia and PD, respectively.[28] We postulated that D1R region-specific pharmacology could be achieved by exploiting the contrasting localizations of $G\alpha_s$ and $G\alpha_{olf}$, the two highly homologous G-proteins coupled with D1R. Specifically, $G\alpha_{olf}$ is highly segregated and enriched in the striatal regions, while $G\alpha_s$ is largely missing in the striatum and expressed in other areas such as the cortex.[29] We previously identified a compound with efficacy bias toward $G\alpha_s$ over $G\alpha_{olf}$ that showed differential neuromodulatory effects in the cortex or striatum.[30] Furthermore, the G protein subtype selectivity profile appeared to be promising for therapeutic development of dopamine receptors[31,32] and translatable to the behavior of the tested animals.[30,33] Here, we characterized structurally distinct D1R agonists for their transducer activation properties in cells, brain slices, and behavior. Our findings shed light on the conformational differences of D1R that transduce the activation of these two G proteins and the potential utility of separate targeting.

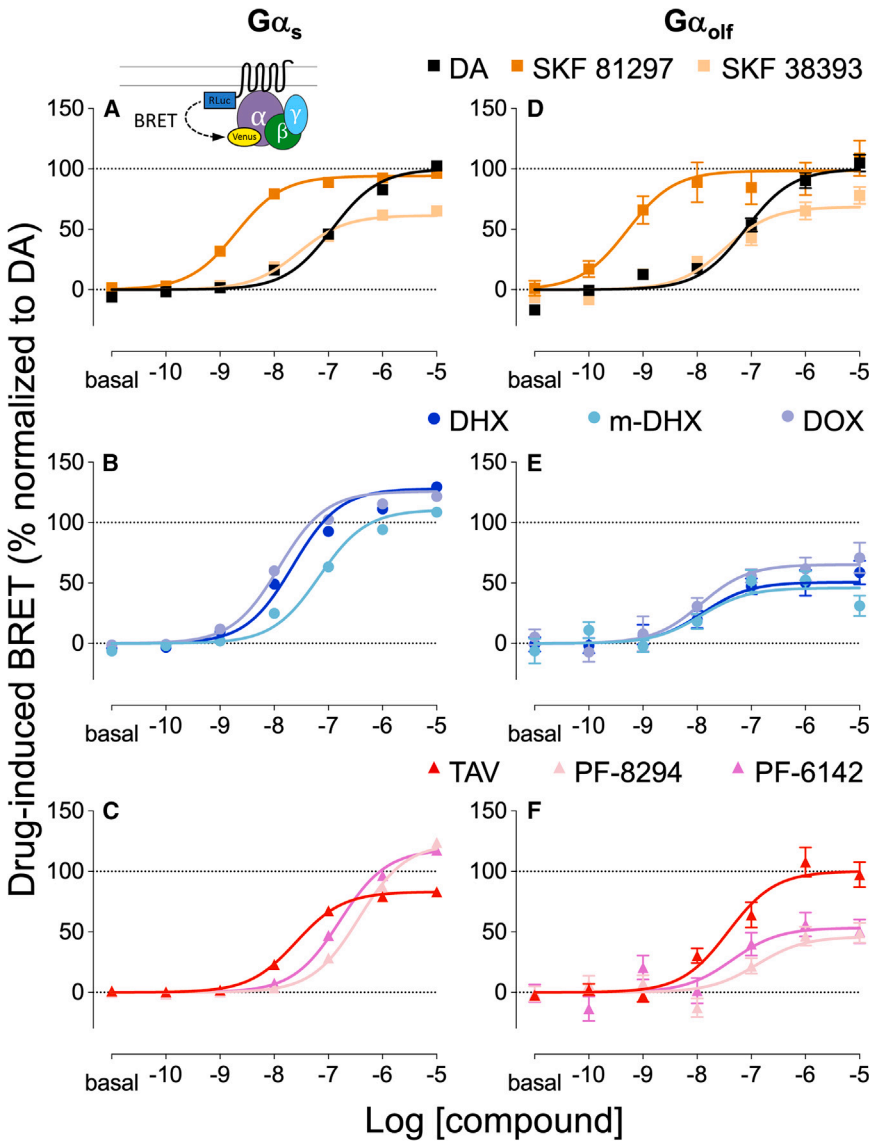

Figure 1. D1R agonist-induced D1R-Gα_s and -Gα_{olf} engagement

Drug-induced BRET ratio change between D1R-Rluc8 and Gα_s-Venus (A–C) or Gα_{olf}-Venus (D–F) in response to DA (black), SKF 81297 (dark orange), SKF 38393 (light orange) (top row), DHX (blue), m-DHX (light blue), DOX (violet) (middle row), TAV (red), PF-8294 (pink), and PF-6142 (magenta). Results were normalized to the E_{max} of DA response for D1R-Gα_s (A–C) and D1R-Gα_{olf} (D–F) and presented as mean ± SEM ($n \geq 5$).

RESULTS

D1R agonists with differential efficacy at Gα_s or Gα_{olf} were identified in D1R-G protein engagement and activation assays

We used receptor-Gα engagement bioluminescence resonance energy transfer (BRET), Gα-γ activation BRET, and the fluorescence-based cAMP biosensor Pink Flamindo to study three main stages of activation: (1) conformational change within the receptor to accommodate the G protein upon agonist binding, (2) subunit rearrangement/dissociation of heterotrimeric G protein following the GTP-GDP exchange, and (3) activation of immediate signaling effector.

Inference about the full or partial agonism of one ligand was made based on a reference compound, usually the endogenous ligand of the receptor studied. For all cell-based assays, DA was used as the reference and the efficacy of all ligands tested was normalized to that of DA in the same condition. In addition, SKF 81297 and SKF 38393, the established full and partial D1R agonists, respectively, were used to validate the assays' sensitivity. As expected, SKF 81297 was as effective as DA in recruiting and activating both G proteins whereas SKF 38393 demonstrated significantly lower efficacy in both BRET configurations used (Figures 1A, 1D, 2A, and 2D).

In this study, we investigated a series of D1R agonists with diverse structures from both catechol (dihydrexidine [DHX], methyl-dihydrexidine [m-DHX], doxanthrine[DOX])[34] and non-catechol (tavapadon [TAV], PF-8294, PF-6142)[19] classes (Figure S1). Unlike the control compounds (i.e., DA, SKF38393, SKF81297), there was a discernible difference in the efficacy of these agonists relative to DA at Gα_s and Gα_{olf}. Of the compounds tested, DHX, m-DHX, DOX, PF-8294, and PF-6142 exerted full agonism at recruiting Gα_s, evidenced by their comparable or significantly higher efficacy at Gα_s, but acted as partial agonists in Gα_{olf} engagement. Interestingly, TAV induced Gα_{olf} coupling with efficacy comparable to DA but was significantly less efficacious at Gα_s recruitment (Figures 1B, 1C, 1E, and 1F; Table S1). Consistent with the results obtained from engagement BRET, the efficacy and potency of these agonists were retained when they were tested in activation BRET (Figures 2B, 2C, 2E, and 2F; Table S2). TAV remained the only compound that behaved as a full agonist at Gα_{olf} activation whereas the rest of the compounds showed a clear preference for activating Gα_s over Gα_{olf}.

Gα_s-Gα_{olf} subtype selectivity was consistently seen in G protein function at cAMP production level

Activation of adenylyl cyclase (AC) via Gα_s and Gα_{olf} to increase cAMP is the major signaling pathway mediated by D1R. Thus, drug-induced cAMP production was studied to evaluate Gα_s and Gα_{olf} activities at the functional level using the red-shifted fluorescence-based biosensor Pink Flamindo.[35]

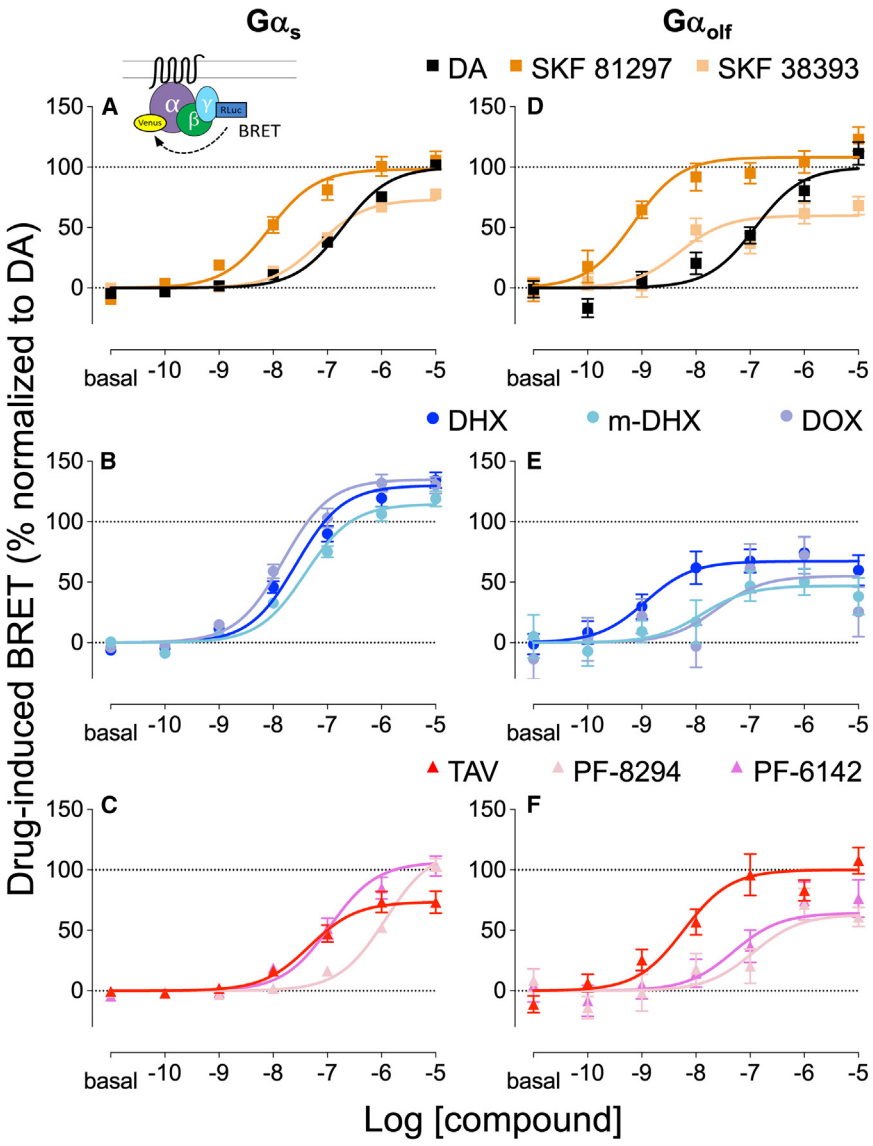

Figure 2. D1R agonist-induced D1R-Gα_s and -Gα_{olf} activation

Drug-induced BRET ratio change between γ7-Rluc8 and Gα_s-Venus (A–C) or Gα_{olf}-Venus (D–F) in response to DA (black), SKF 81297 (dark orange), SKF 38393 (light orange) (top row), DHX (blue), m-DHX (light blue), DOX (violet) (middle row), TAV (red), PF-8294 (pink), and PF-6142 (magenta). Results were normalized to the E_{max} of DA response for D1R-Gα_s (A–C) and D1R-Gα_{olf} (D–F) and presented as mean ± SEM ($n \geq 5$).

Both full and partial benzazepine catechol agonists (SKF 81297 and SKF 38393) showed a consistent efficacy level in promoting cAMP production relative to DA as the G protein engagement or activation assays (Figures 1A, 1D, 2A, 2D, 3A, and 3D). The tetracyclic catechol compounds were equally efficacious to DA at Gα_s but were significantly less effective at Gα_{olf} (Figures 3B and 3E). Similar to the G protein engagement and activation assays, PF-8294 and PF-6142 showed full and partial agonism in Gα_s- and Gα_{olf}-mediated cAMP production, respectively, whereas TAV behaved as a partial agonist at Gα_s and a full agonist at Gα_{olf} (Figures 3C and 3F; Table S3). In addition, potency ranking was similar among G protein engagement, activation, and cAMP production assays as with SKF 81297 and PF-8294 being the most and least potent, respectively, for both Gα_s and Gα_{olf}. Furthermore, SKF 38393, DHX, m-DHX, DOX, and TAV were all within 0.8 Log[EC50] separation for each assay (Tables S1–S3).

Receptor reserve is known to confound D1R agonists' intrinsic activity in molecular expression systems where the receptors are overexpressed.[36–38] To address this concern, SKF81297, SKF 38393, DHX, and TAV were used in a cAMP production assay in which the amount of D1R transfected was lowered by 40 times and cells were treated with N-ethoxycarbonyl-2-ethoxy-1,2-dihydroquinoline (EEDQ), an alkylating agent as an irreversible dopamine receptor antagonist, to further reduce the number of D1Rs expressed. While the E_{max} of these agonists was lowered in the presence of EEDQ, their relative differences in efficacy were maintained, as seen in the experiments where EEDQ was absent. (Figure S2). This suggested that the intrinsic activities reported for these compounds were indeed true in a physiological environment. Taken together, our assays presented a distinct profile in G-protein activation of DHX, m-DHX, DOX, TAV, PF-8294, and PF-6142 at two highly homologous transducers, Gα_s and Gα_{olf}, suggesting the possibility of developing compounds that selectively target one subtype.

Pharmacological profiles for β-arrestin 1 and 2 recruitment were distinct from G protein engagement

β-arrestin-mediated G protein-coupled receptor (GPCR) internalization is a well-characterized mechanism regulating signal transduction.[39] In addition, β-arrestin also acts as a scaffold to recruit components of other signaling pathways independent of G-proteins.[40] Here, we used BRET to study β-arrestin recruitment by these D1R agonists. As β-arrestin 1 and β-arrestin 2 are widely expressed in the CNS, we evaluated these compounds' activity at both subtypes relative to DA. SKF 38393 showed minimal recruitment of both β-arrestin 1 and 2 (22% and 28%, respectively, Figures S3A and S3D; Table S4). SKF 81297 was significantly less efficacious than DA in recruiting β-arrestin 1 and 2 (44% and 82%, respectively, Figures S3A and S3D;

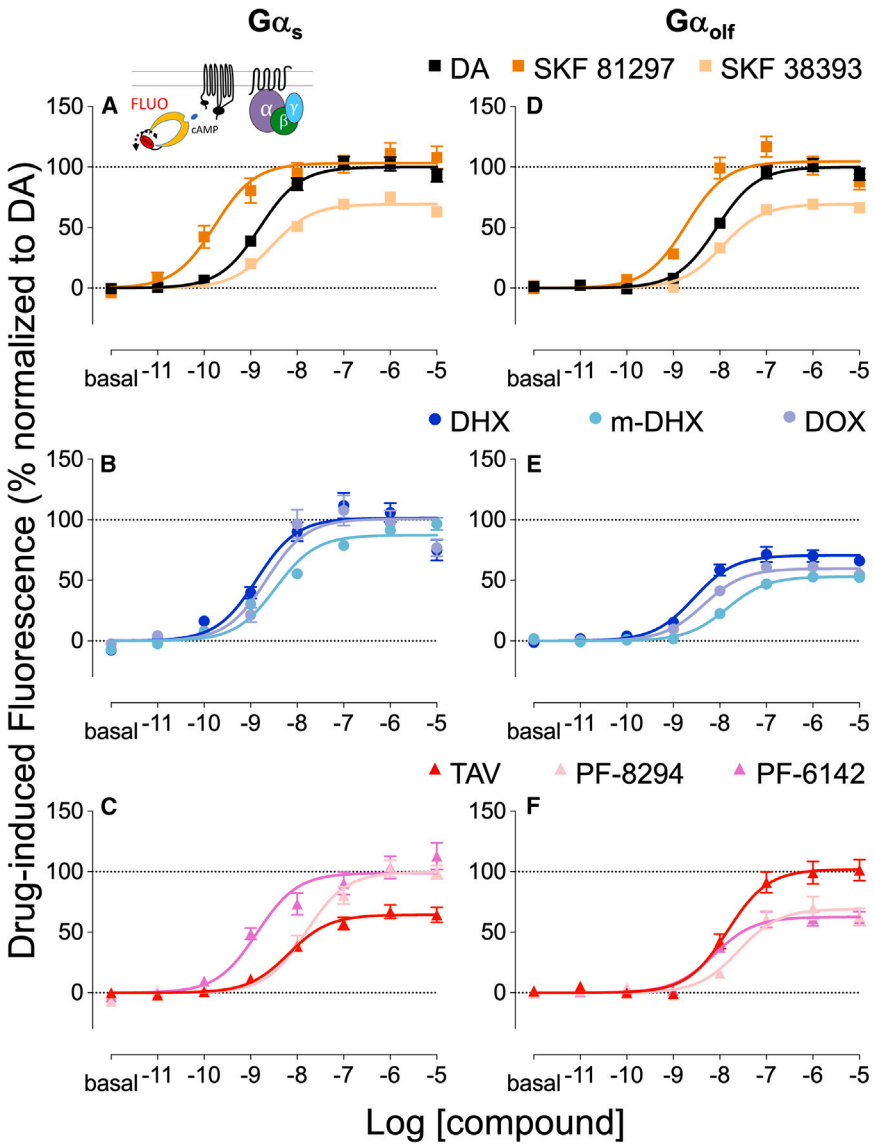

Figure 3. D1R agonist-induced cAMP production via $G\alpha_s$ and $G\alpha_{olf}$

Drug-induced fluorescence change of the cAMP biosensor Pink Flamindo in D1R-$G\alpha_s$ (A–C) or D1R-$G\alpha_{olf}$ (D–F) in response to DA (black), SKF 81297 (dark orange), SKF 38393 (light orange) (top row), DHX (blue), m-DHX (light blue), DOX (violet) (middle row), TAV (red), PF-8294 (pink), and PF-6142 (magenta). Results were normalized to the E_{max} of DA response for D1R-$G\alpha_s$ (A–C) and D1R-$G\alpha_{olf}$ (D–F) and presented as mean ± SEM ($n \geq 5$).

Table S4). These benzazepine catechol compounds showed G-protein bias, as reported previously.[41]

With the exception of m-DHX at β-arrestin 1 recruitment (70%) (Figure S3B), the tetracyclic catechol compounds demonstrated a high level of β-arrestin recruitment for both subtypes. Compared to their efficacy at $G\alpha_s$ engagement BRET assay, DHX, m-DHX, and DOX appeared to be balanced agonists at these two transducers (Figures S3B and S3E). In contrast, the efficacy of the non-catechol compounds at β-arrestin 1 and 2 recruitment was significantly lower than that of DA (Figures S3C and S3F). Cross-comparison with their E_{max} values at $G\alpha_s$ coupling revealed a clear bias for G-protein engagement of TAV, PF-8294, and PF-6142.

αN swap in $G\alpha_{olf}$ chimera partially mimicked $G\alpha_s$ activity

Recent cryo-EM structure studies suggested the receptor-G-protein interacting domains that contribute to the G protein subtype selectivity among different dopamine receptors.[42–44] Of the domains involved at the interface, intracellular loop 2 (ICL2) of D1R appeared to play a crucial role in this selectivity and was within interacting distance with the αN domain of the G protein (Figures 4A and 4B).[20] Previously, by substituting six amino acids in the αN helix of $G\alpha_{olf}$ (ERLAYK) with the $G\alpha_s$ equivalent residues (DKQVYR) (Figures 4B and S4), referred to as $G\alpha_{olf}$ αN, we were able to partially restore the $G\alpha_s$ selectivity of DHX in engagement BRET.[30] Here, we used the untagged $G\alpha_{olf}$ αN and monitored the effect of this substitution at the functional level. Compared to their effects in wild-type (WT) $G\alpha_s$ and $G\alpha_{olf}$ (Figures 3A and 3B), SKF 81297 and SKF 38393 retained their relative efficacy and potency in cAMP production in $G\alpha_{olf}$ αN (Figure 4C). However, there is a clear difference in the efficacy of the other compounds when tested with the $G\alpha_{olf}$ αN chimera. The tetracyclic catechol compounds (DHX, m-DHX, and DOX) significantly increased the cAMP production compared to their performance in WT $G\alpha_{olf}$, approaching the level seen in WT $G\alpha_s$ (Figures 4D and S5B).

The effect of this substitution appeared to be more profound in the non-catechol compounds. We noticed the same trend in PF-8294 and PF-6142 where the efficacy in $G\alpha_{olf}$ αN was significantly enhanced from their E_{max} in WT $G\alpha_{olf}$. Strikingly, PF-8294 efficacy in $G\alpha_{olf}$ αN was comparable to that in WT $G\alpha_s$. TAV was the only $G\alpha_{olf}$-selective compound in this set. When tested with $G\alpha_{olf}$ αN, TAV was significantly less efficacious in producing cAMP than it was in WT $G\alpha_{olf}$. In addition, TAV efficacy in $G\alpha_{olf}$ αN was not different from that of $G\alpha_s$ (Figures 4E and S5C).

D1R-mediated enhancement of pathway-specific synaptic events was seen with varied efficacy levels

Based on the distinct distribution of $G\alpha_s$ and $G\alpha_{olf}$ in the CNS, $G\alpha_s$-selective D1R agonists are expected to exert higher efficacy in

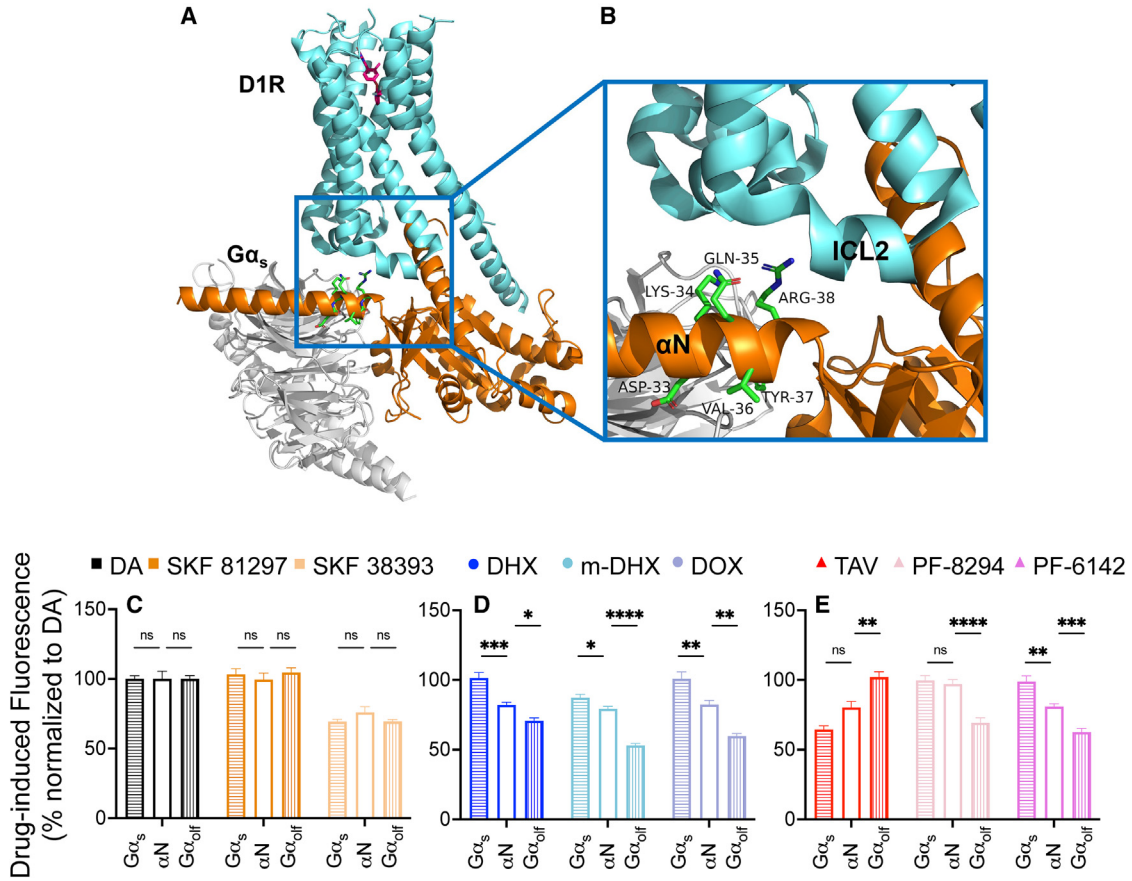

Figure 4. D1R agonist-induced cAMP production via $G\alpha_{olf/s}$ chimera

(A) Cryo-EM structure of TAV-bound D1R and mini-$G\alpha_s$ complex (PDB: 7X2D).

(B) The ICL2-αN interface of the D1R-$G\alpha_s$ complex. Molecular graphics were generated in PyMOL 3.1. Drug-induced fluorescence change of Pink Flamindo detecting cAMP level for DA (black), SKF81297 (orange), SKF38393 (light orange) (C), DHX (blue), m-DHX (light blue), DOX (violet) (D), TAV (red), PF-8294 (pink), and PF-6142 (magenta) (E). Results were normalized to the E_{max} of DA response for $G\alpha_s$, $G\alpha_{olf/s}$ chimera (αN), $G\alpha_{olf}$ and presented as mean ± SEM ($n \geq 5$). Comparison of the E_{max} across $G\alpha_s$, αN, and $G\alpha_{olf}$ was done using one-way ANOVA followed by post-hoc Tukey test.

*, **, ***, ****$p < 0.05$, 0.01, 0.001, 0.0001, respectively.

modulating cortex-related electrophysiological events, whereas compounds that induce better $G\alpha_{olf}$ coupling may preferentially modulate events that are associated with the striatum. The thalamus is one of the major sources of glutamate input to the cortex where it triggers cortical excitatory post-synaptic current (EPSC) via N-methyl-D-aspartate receptors (NMDAR). As D1R has been reported to potentiate the EPSC in the mPFC, recording EPSCs from the cortical pyramidal cells in the presence of D1R agonists may reveal NMDAR potentiation by D1R.[45–47] By contrast, activation of D1Rs at either axons or synaptic terminals of striatal medium spiny neurons (MSN) has been reported to presynaptically facilitate the substantia nigra pars reticulata (SNr) inhibitory postsynaptic current (IPSC).[48–50] Thus, monitoring the IPSC of SNr γ-aminobutyric acid (GABA)-ergic cells can allow evaluation of D1R pharmacology of D1R-expressing MSN afferents through the degree of enhanced response.[51,52]

Here, we combined optical stimulation of channelrhodopsin-2 (ChR2)[53] and whole-cell voltage clamp on mouse brain slices to investigate D1R agonists' effects on synaptic transmission in the thalamocortical and striatonigral projections. AAV5-hSyn-hChR2(H134R)-EYFP was stereotaxically injected into the mediodorsal thalamus of *Drd1a*-tdTomato BAC transgenic mice for the expression in the thalamocortical pathway. In turn, the virus was injected into the dorsal lateral striatum of WT mice for the striatonigral pathway. Three weeks post-surgery, ChR2 was successfully expressed, evidenced by the strong expression of yellow fluorescence in the cortex (Figure 5A) or the SNr (Figure 5D). D1R-expressing pyramidal cells in mPFC elicited an EPSC upon blue LED light stimulation. When the slices were perfused with 1 μM SKF 81297, the EPSC peak amplitude significantly increased (113.4% of baseline, $p < 0.01$). The same results were observed when the slices were perfused with 1 μM DHX (113.1% of baseline, $p < 0.05$). However, perfusing 1 μM tavapadon did not enhance the cortical EPSC amplitude (Figures 5B and 5C). The EPSC potentiation effect of SKF 81297 was abrogated when the slices were concurrently perfused with 10 μM SCH 23390, a selective D1R antagonist, and 1 μM SKF 81297 (Figures S6A and S6B), showing the specificity of D1R-mediated EPSC effect.

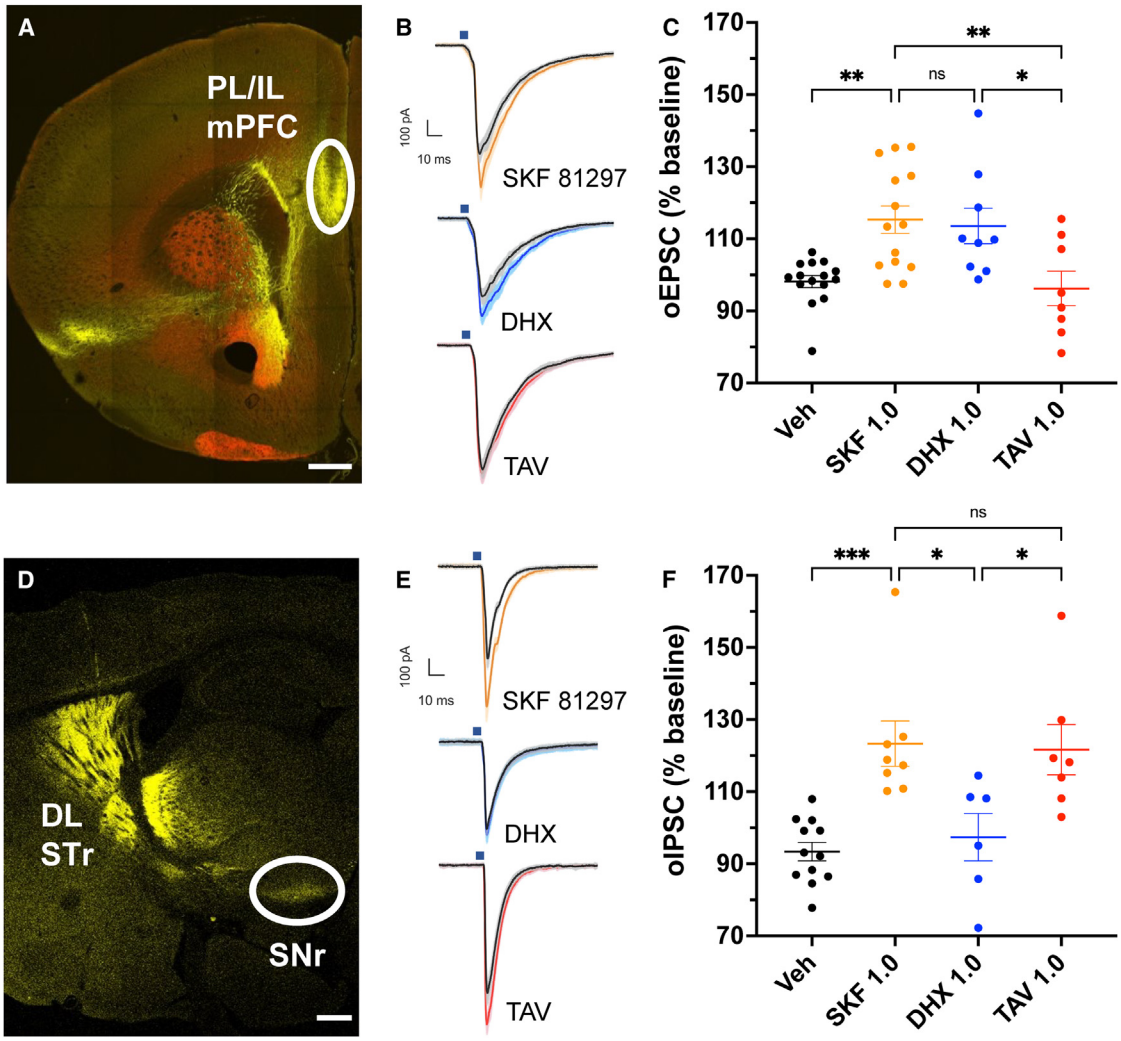

Figure 5. $G\alpha_s$ and $G\alpha_{olf}$ activities in brain slice electrophysiology

ChR2-YFP injection in the mediodorsal thalamus projecting to the prelimbic/infralimbic mPFC of D1R-tdTomato mouse (A) and in the dorsal striatum projecting to the SNr of WT mouse (D). Scale bar: 500 μm. Average traces of the optically elicited ChR2-driven EPSCs in the mPFC (B) and IPSCs in the SNr (E) following 2 ms of photostimulation by blue light. Analysis of the D1R-mediated potentiation of EPSCs in the mPFC (C) IPSCs in the SNr (F) for 1.0 μM SKF81297, DHX, and TAV (orange, blue, and red) was done using one-way ANOVA followed by post-hoc Tukey test.

*, **, ***$p < 0.05$, 0.01, 0.001 respectively.

Photostimulation of the MSN GABAergic afferent in the SNr elicited an IPSC that was markedly enhanced by 1 μM SKF 81297 (123.3% of baseline, $p < 0.01$). This SKF 81297 effect was antagonized by SCH 23390 (Figures S6C and S6D). In contrast to its effect in the mPFC, 1 μM tavapadon significantly potentiated the IPSC in the SNr (123.1% of baseline, $p < 0.05$). This effect was comparable to that seen with SKF 81297. DHX, on the other hand, failed to modulate the IPSC in the SNr (Figures 5E and 5F). The electrophysiological effects seen from the recordings with DHX and TAV were consistent with their selectivity profiles *in vitro* (Figures 1, 2, and 3). This finding suggested that D1R agonists that preferentially activate one G protein subtype might be able to selectively modulate the electrophysiological events in the area where that G protein is enriched, indicating that D1R region-specific pharmacology can be achieved by targeting the G-protein subtypes.

Locomotor rescue in cataleptic mice revealed a significant difference in efficacy between tavapadon and dihydrexidine

D1R in the striatum regulates locomotor activity, likely via $G\alpha_{olf}$, due to its high level of expression in this brain region.[54] The psychostimulatory effect of D1R agonists reflects this $G\alpha_{olf}$-mediated striatal function. However, endogenous DA can be a potential confounding factor in studying this effect *in vivo* as it can mask the effects of D1R agonists via D1R in both the striatum and elsewhere. Therefore, it is necessary to deplete the endogenous DA levels to elicit an akinetic state so that D1R agonist

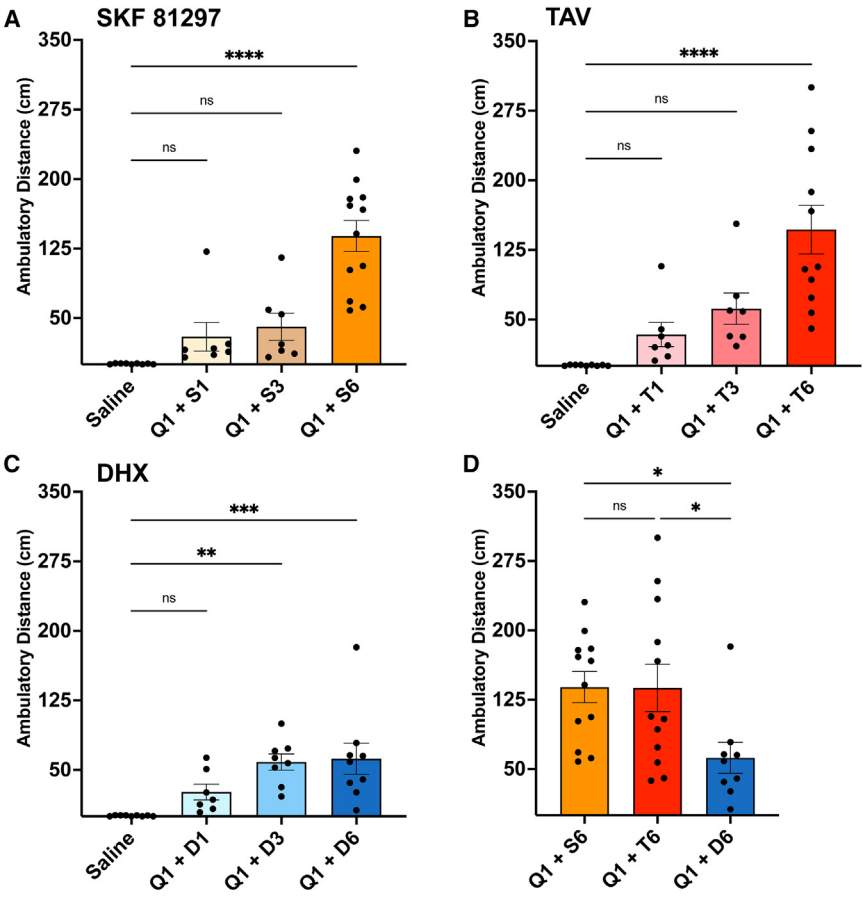

Figure 6. D1R agonists effect on locomotor activity

(A–C) Psychomotor stimulatory effect of SKF-81297 [S] (A), TAV [T] (B), and DHX [D] (C) at 1, 3, 6 mg/kg (S1, S3, S6 etc.) in combination with 1 mg/kg quinpirole (Q1) on DA-depleted reserpinized mice.

*, **, ***, ****$p < 0.05$, 0.01, 0.001, 0.0001, respectively, compared to the effect of saline using one-way ANOVA followed by post-hoc Dunnett test.

(D) Comparison of the ambulatory distance induced by these drugs at 6 mg/kg was done using one-way ANOVA followed by post-hoc Tukey test.

*, **, ***, ****$p < 0.05$, 0.01, 0.001, 0.0001, respectively.

effects in the striatal neurons can be studied effectively as widely reported for DA drugs.[55–57] To that end, reserpine was used to irreversibly block the vesicular monoamine transporters 1 and 2 (VMAT-1 and VMAT-2), rendering the depletion of DA in the synaptic terminals.[58]

SKF 81297, DHX, and TAV induced significant locomotor stimulation in a dose-dependent manner (Figures 6A–6C). At the highest tested dose (6 mg/kg), the effects of TAV and SKF 81297 were comparable. Interestingly, DHX was significantly less efficacious than either of the aforementioned drugs in stimulating locomotor activity (44.79% of SKF 81297 and 45.09% of TAV) (Figure 6D). That is in line with our *in vitro* and *ex vivo* data and suggests that $G\alpha_{olf}$-selective D1R agonists might be better at rescuing locomotor activity, probably due to their preferential stimulation of D1Rs in the striatum.

Tavapadon and dihydrexidine exhibited distinct effectiveness in enhancing cognitive function in mice

D1Rs in the mPFC serve a crucial role in mediating cognitive and executive functions, as well as social behaviors.[59–61] As $G\alpha_s$ is predominant in the mPFC, we hypothesized that $G\alpha_s$-selective compounds would better modulate the behavior associated with this region. To investigate the cognitive effect of these pharmacological agents, the novel object recognition (NOR) assay was chosen due to its robustness and high sensitivity.[62–64]

Mice that received 6 mg/kg SKF 81297 showed a significantly higher discriminatory index (DI = 0.38) than the saline-injected group (DI = 0.05). As expected, 6 mg/kg DHX exhibited comparable efficacy to SKF 81297 in enhancing the cognitive function of the mice (DI = 0.33), while 6 mg/kg TAV was significantly less effective (DI = 0.07) (Figure 7). In addition, the drugs did not alter the locomotor activity of the mice (data not shown), indicating that the increase in DI observed was indeed due to the enhancement in cognitive function. These results are consistent with the functional selectivity profiles *in vitro* and the electrophysiological effects of these compounds, corroborating the hypothesis that $G\alpha_s$-selective D1R agonists would be more effective in modulating cognitive functions.

DISCUSSION

It has been reported that the restricted conformation of the β-phenyl-dopamine pharmacophore renders the selectivity and full agonism at D1R of catechol D1R agonists.[34] Here, we expanded on this finding and revealed a differential activation profile of DHX, m-DHX, and DOX at two homologous G protein subtypes, $G\alpha_s$ and $G\alpha_{olf}$. Although these compounds exerted full agonism at $G\alpha_s$, they behaved as partial agonists at $G\alpha_{olf}$ (Figures 1, 2, and 3). This characteristic was discernibly different from that of the benzazepine catechol D1R agonists, where the β-phenyl ring is not restricted. We surmised the rigid ring structure of these compounds might contribute to the activity bias toward $G\alpha_s$.

A series of arylphenoxyaryl D1R agonists was developed in recent years and their structure-activity relationships have been studied by several groups. Modifications of the two heterocyclic groups at the ends or the core linking structure could drastically alter the selectivity of these compounds between G protein and β-arrestin signaling.[18,19,26,27] Replacing the trifluoromethyl pyridine ring of TAV with the pyridofuran ring of PF-8294 and PF-6142 increased potency in the cAMP production assay and

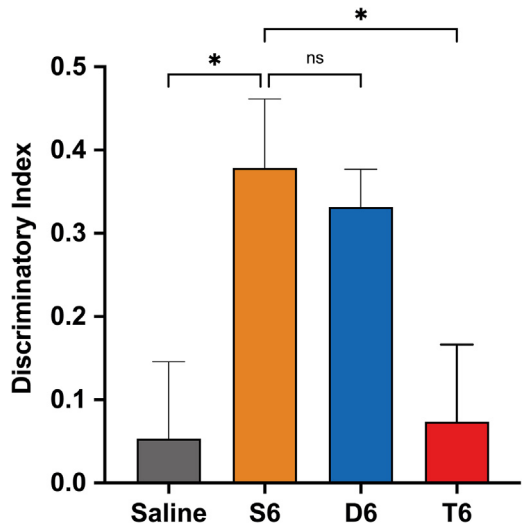

Figure 7. D1R agonists effect on cognitive function using the novel object recognition assay

Comparison of the discriminatory index (DI) of WT mice following the administration of SKF-81297 [S6], TAV [T6], and DHX [D6] at 6 mg/kg $*p < 0.05$ compared to the SKF 81297-injected group using one-way ANOVA followed by post-hoc Dunnett test.

also enhanced both efficacy and potency in the β-arrestin recruitment assay.[26] By contrast, substituting the imidazopyridine ring of PF-8294 with the imidazopyrazine ring of PF-6142 at a different attachment position increased efficacy and potency in the cAMP production assay, but did not cause a significant change in the β-arrestin recruitment assay.[19,27] These findings align with our current data on $G\alpha_s$-mediated cAMP production and β-arrestin recruitment (Figures 3C and S3). To our knowledge, we are the first to report the profiles of these compounds at $G\alpha_s$ and $G\alpha_{olf}$. Interestingly, TAV, PF-8294, and PF-6142 consistently showed differential activities at these two G proteins. Although PF-8294 and PF-6142 demonstrated selectivity toward $G\alpha_s$, TAV was selective toward $G\alpha_{olf}$. This suggests that by substituting the heterocyclic groups of the arylphenoxyaryl pharmacophore, in addition to altering the G protein—β-arrestin relationship, subtype selectivity can also be modified. This finding is significant given the unique expression pattern of $G\alpha_s$ and $G\alpha_{olf}$ in the CNS and the behaviors associated with these regions.

The β-arrestin-mediated GPCR internalization accounts for developing drug tolerance.[65] The high efficacy at β-arrestin recruitment of DHX, m-DHX, and DOX (Figures S3B and S3E) might explain the rapid tolerance usually seen with tetracyclic catechol D1R agonists.[16] Our results on β-arrestin recruitment of PF-8294 and PF-6142 (Figures S3C and S3F) agreed with the previously published data regarding the reduced desensitization of D1R upon drug exposure.[27] Furthermore, the low β-arrestin recruitment of TAV could be one reason for this compound's improved tolerability in clinical trials.[23]

Our previous publication showed that the αN/IL2 (Gα/D1R) interface contributes to the G protein subtype selectivity of these compounds.[30] Although the chimeric construct $G\alpha_{olf}$ αN significantly altered the efficacy of these compounds trending toward $G\alpha_s$, their potency remained unchanged from WT $G\alpha_{olf}$ (Table S3), suggesting that other domains might also contribute to G protein subtype selectivity. Despite the high degree of homology, there are domains with divergent amino acid sequences between $G\alpha_s$ and $G\alpha_{olf}$, especially at the regions interfacing D1R (Figure S4). A more thorough analysis of subdomains is warranted and currently underway.

Our electrophysiology data indicate a pathway-specific effect of DHX and TAV. We expected that selective targeting of G protein subtype via D1R would allow modulation of the neurological and neuropsychiatric outcomes associated with that region. Specifically, cortical D1R has a significant role in regulating executive functions and working memory,[8,10,66] whereas striatal D1R is one of the main players in voluntary movements, reward, and motivation.[4,5,7,67–69] Thus, region-specific G protein activation via D1R will have great implications for developing treatments for several disorders, such as cognitive deficiency and movement disorder, while potentially limiting the adverse off-target effects from globally activating all the D1Rs in the brain.

Developing D1R agonists, especially ones with the catechol moiety, has been proven to be challenging due to appreciable adverse effects. It has been reported that some compounds are epileptogenic or can decrease seizure thresholds.[70,71] In addition, cardiovascular effects are the other concern regarding the safety of these agonists. In fact, hypotension prevented several compounds from advancing to later phases of clinical trials,[14,16] which might be due to the off-target effects of these drugs on peripheral D1Rs.[72] Some degrees of seizures were observed in a few mice when tested at 6 mg/kg of SKF 81297, although this phenomenon was not observed with DHX and especially $G\alpha_{olf}$-biased TAV, even at 10 mg/kg (data not shown).

Based on our *in vitro* and electrophysiology results, we expected that DHX and TAV might exhibit different efficacy in controlling the mPFC-mediated cognitive function and the striatum-mediated locomotor activity. Indeed, our results on locomotor rescue of these D1R agonists on DA-depleted mice showed a significantly higher efficacy of TAV compared to DHX (Figure 6D). In contrast, the data from the NOR assay indicated that DHX was more effective than TAV in improving the cognitive function of the tested mice (Figure 7). These findings were particularly interesting because they corroborated our hypothesis that it would be possible to selectively activate D1Rs in different brain regions by exploiting the unique expression pattern of $G\alpha_s$ and $G\alpha_{olf}$ in the CNS, thereby allowing manipulation of selective physiological functions controlled by one particular brain region or cell-type.

Overall, our study suggested that the *in vitro* G protein subtype selectivity profile of D1R agonists is translatable to their physiological effects. The current study design is a reliable model to screen for compounds with different clinical significance. The results reported at various physiological levels herein consistently showed that TAV had a unique efficacy bias toward $G\alpha_{olf}$ whereas PF-8294, PF-6142 and the DHX analogs series showed a $G\alpha_s$ efficacy bias.

Limitations of the study

This study focused on the G-protein subtype selectivity of D1R and its potential clinical application in several neurological and neuropsychiatric disorders. While the data corroborated the

notion that $G\alpha_s$-selective agonists would be more beneficial in treating cognitive deficiency and $G\alpha_{olf}$-selective agonists would have more desirable outcomes in the treatment of movement disorders, we are aware that cognitive functions and locomotor activity are far more complex and nuanced. More models, therefore, should be used to investigate the behavioral effects of the evaluated biased drugs. In addition, studying the drug effects following chronic use as opposed to single use would be more clinically relevant. Lastly, we discovered that the six residues at the C terminus of the αN domain of the G proteins contributed to this subtype selectivity. However, since the receptor-G-protein interface also involves other domains, such as α4 and α5, investigating these domains will further elucidate the molecular mechanism underlying this phenomenon.

RESOURCE AVAILABILITY

Lead contact

Further information and requests for reagents should be directed to the lead contact, Hideaki Yano (h.yano@northeastern.edu).

Materials availability

Plasmids generated in this study are available upon request or have been deposited to Addgene as indicated in the key resources table.

Data and code availability

- All data are included in the manuscript. Microscopy data reported in this paper will be shared by the lead contact upon request.
- This paper does not generate any original codes.
- Any additional information required to reanalyze the data reported in this paper is available from the lead contact upon request.

ACKNOWLEDGMENTS

PF-8294 and PF-6142 compounds were provided under a Material Transfer Agreement with F. Hoffmann-La Roche LTD (Basel, Switzerland). The work was supported by Northeastern University Startup Funds and Tier1 Intramural Grant (H.Y.). AI was funded by KAKENHI JP21H04791, JP21H05113, and JP21H05037 from the Japan Society for the Promotion of Science; JP22ama121038 and JP22zf0127007 from the Japan Agency for Medical Research and Development; JPMJFR215T and JPMJMS2023 from the Japan Science and Technology Agency. Graphical abstract was made with BioRender.com.

AUTHOR CONTRIBUTIONS

H.Y. conceptualized the study. A.M.N., A.S., and V.Q. designed and carried out the experiments and performed the data analysis with H.Y.; AI provided $G\alpha_{s/olf}$-KO HEK 293A cells; D.E.N. provided tetracyclic catechol D1R agonists; A.M.N. and H.Y. prepared the initial manuscript, with contributions from all the authors in finalizing the manuscript.

DECLARATION OF INTERESTS

The authors declare no competing financial interests.

STAR★METHODS

Detailed methods are provided in the online version of this paper and include the following:

SUPPLEMENTAL INFORMATION

Supplemental information can be found online at https://doi.org/10.1016/j.isci.2025.112345.

Received: April 5, 2024
Revised: January 2, 2025
Accepted: March 31, 2025
Published: April 3, 2025

REFERENCES

1. De Keyser, J., Claeys, A., De Backer, J.P., Ebinger, G., Roels, F., and Vauquelin, G. (1988). Autoradiographic localization of D1 and D2 dopamine receptors in the human brain. Neurosci. Lett. *91*, 142–147. https://doi.org/10.1016/0304-3940(88)90758-6.
2. Hegarty, S.V., Sullivan, A.M., and O'Keeffe, G.W. (2013). Midbrain dopaminergic neurons: a review of the molecular circuitry that regulates their development. Dev. Biol. *379*, 123–138. https://doi.org/10.1016/j.ydbio.2013.04.014.
3. Beaulieu, J.M., and Gainetdinov, R.R. (2011). The physiology, signaling, and pharmacology of dopamine receptors. Pharmacol. Rev. *63*, 182–217. https://doi.org/10.1124/pr.110.002642.
4. Waszczak, B.L., Martin, L.P., Finlay, H.E., Zahr, N., and Stellar, J.R. (2002). Effects of individual and concurrent stimulation of striatal D1 and D2 dopamine receptors on electrophysiological and behavioral output from rat basal ganglia. J. Pharmacol. Exp. Ther. *300*, 850–861. https://doi.org/10.1124/jpet.300.3.850.
5. Vermeulen, R.J., Drukarch, B., Sahadat, M.C., Goosen, C., Wolters, E.C., and Stoof, J.C. (1994). The dopamine D1 agonist SKF 81297 and the dopamine D2 agonist LY 171555 act synergistically to stimulate motor behavior of 1-methyl-4-phenyl-1,2,3,6-tetrahydropyridine-lesioned parkinsonian rhesus monkeys. Mov. Disord. *9*, 664–672. https://doi.org/10.1002/mds.870090613.
6. Halbout, B., Marshall, A.T., Azimi, A., Liljeholm, M., Mahler, S.V., Wassum, K.M., and Ostlund, S.B. (2019). Mesolimbic dopamine projections mediate cue-motivated reward seeking but not reward retrieval in rats. Elife *8*, e43551. https://doi.org/10.7554/eLife.43551.
7. Kravitz, A.V., Tye, L.D., and Kreitzer, A.C. (2012). Distinct roles for direct and indirect pathway striatal neurons in reinforcement. Nat. Neurosci. *15*, 816–818. https://doi.org/10.1038/nn.3100.
8. Wulaer, B., Kunisawa, K., Tanabe, M., Yanagawa, A., Saito, K., Mouri, A., and Nabeshima, T. (2021). Pharmacological blockade of dopamine D1- or D2-receptor in the prefrontal cortex induces attentional impairment in the object-based attention test through different neuronal circuits in mice. Mol. Brain *14*, 43. https://doi.org/10.1186/s13041-021-00760-3.
9. Puig, M.V., and Miller, E.K. (2015). Neural Substrates of Dopamine D2 Receptor Modulated Executive Functions in the Monkey Prefrontal Cortex. Cereb. Cortex *25*, 2980–2987. https://doi.org/10.1093/cercor/bhu096.
10. Rinaldi, A., Mandillo, S., Oliverio, A., and Mele, A. (2007). D1 and D2 receptor antagonist injections in the prefrontal cortex selectively impair spatial learning in mice. Neuropsychopharmacology *32*, 309–319. https://doi.org/10.1038/sj.npp.1301176.

11. Arnsten, A.F., Cai, J.X., Murphy, B.L., and Goldman-Rakic, P.S. (1994). Dopamine D1 receptor mechanisms in the cognitive performance of young adult and aged monkeys. Psychopharmacology (Berl) *116*, 143–151. https://doi.org/10.1007/BF02245056.

12. Taylor, J.R., Lawrence, M.S., Redmond, D.E., Elsworth, J.D., Roth, R.H., Nichols, D.E., and Mailman, R.B. (1991). Dihydrexidine, a full dopamine D1 agonist, reduces MPTP-induced parkinsonism in monkeys. Eur. J. Pharmacol. *199*, 389–391. https://doi.org/10.1016/0014-2999(91)90508-n.

13. Mu, Q., Johnson, K., Morgan, P.S., Grenesko, E.L., Molnar, C.E., Anderson, B., Nahas, Z., Kozel, F.A., Kose, S., Knable, M., et al. (2007). A single 20 mg dose of the full D1 dopamine agonist dihydrexidine (DAR-0100) increases prefrontal perfusion in schizophrenia. Schizophr. Res. *94*, 332–341. https://doi.org/10.1016/j.schres.2007.03.033.

14. Blanchet, P.J., Fang, J., Gillespie, M., Sabounjian, L., Locke, K.W., Gammans, R., Mouradian, M.M., and Chase, T.N. (1998). Effects of the full dopamine D1 receptor agonist dihydrexidine in Parkinson's disease. Clin. Neuropharmacol. *21*, 339–343.

15. Rascol, O., Nutt, J.G., Blin, O., Goetz, C.G., Trugman, J.M., Soubrouillard, C., Carter, J.H., Currie, L.J., Fabre, N., Thalamas, C., et al. (2001). Induction by dopamine D1 receptor agonist ABT-431 of dyskinesia similar to levodopa in patients with Parkinson disease. Arch. Neurol. *58*, 249–254. https://doi.org/10.1001/archneur.58.2.249.

16. Watts, V.J., Lawler, C.P., Gilmore, J.H., Southerland, S.B., Nichols, D.E., and Mailman, R.B. (1993). Dopamine D1 receptors: efficacy of full (dihydrexidine) vs. partial (SKF38393) agonists in primates vs. rodents. Eur. J. Pharmacol. *242*, 165–172. https://doi.org/10.1016/0014-2999(93)90076-t.

17. Close, S.P., Marriott, A.S., and Pay, S. (1985). Failure of SKF 38393-A to relieve parkinsonian symptoms induced by 1-methyl-4-phenyl-1,2,3,6-tetrahydropyridine in the marmoset. Br. J. Pharmacol. *85*, 320–322. https://doi.org/10.1111/j.1476-5381.1985.tb08863.x.

18. Martini, M.L., Liu, J., Ray, C., Yu, X., Huang, X.P., Urs, A., Urs, N., McCorvy, J.D., Caron, M.G., Roth, B.L., and Jin, J. (2019). Defining Structure-Functional Selectivity Relationships (SFSR) for a Class of Non-Catechol Dopamine D1 Receptor Agonists. J. Med. Chem. *62*, 3753–3772. https://doi.org/10.1021/acs.jmedchem.9b00351.

19. Davoren, J.E., Nason, D., Coe, J., Dlugolenski, K., Helal, C., Harris, A.R., LaChapelle, E., Liang, S., Liu, Y., O'Connor, R., et al. (2018). Discovery and Lead Optimization of Atropisomer D1 Agonists with Reduced Desensitization. J. Med. Chem. *61*, 11384–11397. https://doi.org/10.1021/acs.jmedchem.8b01622.

20. Hall, A., Provins, L., and Valade, A. (2019). Novel Strategies To Activate the Dopamine D(1) Receptor: Recent Advances in Orthosteric Agonism and Positive Allosteric Modulation. J. Med. Chem. *62*, 128–140. https://doi.org/10.1021/acs.jmedchem.8b01767.

21. Kozak, R., Kiss, T., Dlugolenski, K., Johnson, D.E., Gorczyca, R.R., Kuszpit, K., Harvey, B.D., Stolyar, P., Sukoff Rizzo, S.J., Hoffmann, W.E., et al. (2020). Characterization of PF-6142, a Novel, Non-Catecholamine Dopamine Receptor D1 Agonist, in Murine and Nonhuman Primate Models of Dopaminergic Activation. Front. Pharmacol. *11*, 1005. https://doi.org/10.3389/fphar.2020.01005.

22. Sohur, U.S., Gray, D.L., Duvvuri, S., Zhang, Y., Thayer, K., and Feng, G. (2018). Phase 1 Parkinson's Disease Studies Show the Dopamine D1/D5 Agonist PF-06649751 is Safe and Well Tolerated. Neurol. Ther. *7*, 307–319. https://doi.org/10.1007/s40120-018-0114-z.

23. Riesenberg, R., Werth, J., Zhang, Y., Duvvuri, S., and Gray, D. (2020). PF-06649751 efficacy and safety in early Parkinson's disease: a randomized, placebo-controlled trial. Ther. Adv. Neurol. Disord. *13*, 1756286420911296. https://doi.org/10.1177/1756286420911296.

24. Papapetropoulos, S., Liu, W., Duvvuri, S., Thayer, K., and Gray, D.L. (2018). Evaluation of D1/D5 Partial Agonist PF-06412562 in Parkinson's Disease following Oral Administration. Neurodegener. Dis. *18*, 262–269. https://doi.org/10.1159/000492498.

25. Young, D., Popiolek, M., Trapa, P., Fonseca, K.R., Brevard, J., Gray, D.L., and Kozak, R. (2020). D1 Agonist Improved Movement of Parkinsonian Nonhuman Primates with Limited Dyskinesia Side Effects. ACS Chem. Neurosci. *11*, 560–566. https://doi.org/10.1021/acschemneuro.9b00589.

26. Martini, M.L., Ray, C., Yu, X., Liu, J., Pogorelov, V.M., Wetsel, W.C., Huang, X.P., McCorvy, J.D., Caron, M.G., and Jin, J. (2019). Designing Functionally Selective Noncatechol Dopamine D1 Receptor Agonists with Potent In Vivo Antiparkinsonian Activity. ACS Chem. Neurosci. *10*, 4160–4182. https://doi.org/10.1021/acschemneuro.9b00410.

27. Gray, D.L., Allen, J.A., Mente, S., O'Connor, R.E., DeMarco, G.J., Efremov, I., Tierney, P., Volfson, D., Davoren, J., Guilmette, E., et al. (2018). Impaired β-arrestin recruitment and reduced desensitization by non-catechol agonists of the D1 dopamine receptor. Nat. Commun. *9*, 674. https://doi.org/10.1038/s41467-017-02776-7.

28. Howes, O.D., McCutcheon, R., Owen, M.J., and Murray, R.M. (2017). The Role of Genes, Stress, and Dopamine in the Development of Schizophrenia. Biol. Psychiatry *81*, 9–20. https://doi.org/10.1016/j.biopsych.2016.07.014.

29. Hervé, D. (2011). Identification of a specific assembly of the g protein golf as a critical and regulated module of dopamine and adenosine-activated cAMP pathways in the striatum. Front. Neuroanat. *5*, 48. https://doi.org/10.3389/fnana.2011.00048.

30. Yano, H., Cai, N.S., Xu, M., Verma, R.K., Rea, W., Hoffman, A.F., Shi, L., Javitch, J.A., Bonci, A., and Ferré, S. (2018). Gs- versus Golf-dependent functional selectivity mediated by the dopamine D1 receptor. Nat. Commun. *9*, 486. https://doi.org/10.1038/s41467-017-02606-w.

31. Von Moo, E., Harpsøe, K., Hauser, A.S., Masuho, I., Bräuner-Osborne, H., Gloriam, D.E., and Martemyanov, K.A. (2022). Ligand-directed bias of G protein signaling at the dopamine D2 receptor. Cell Chem. Biol. *29*, 226–238.e4. https://doi.org/10.1016/j.chembiol.2021.07.004.

32. Bonifazi, A., Yano, H., Guerrero, A.M., Kumar, V., Hoffman, A.F., Lupica, C.R., Shi, L., and Newman, A.H. (2019). Novel and Potent Dopamine D2 Receptor Go-Protein Biased Agonists. ACS Pharmacol. Transl. Sci. *2*, 52–65. https://doi.org/10.1021/acsptsci.8b00060.

33. Wall, M.J., Hill, E., Huckstepp, R., Barkan, K., Deganutti, G., Leuenberger, M., Preti, B., Winfield, I., Carvalho, S., Suchankova, A., et al. (2022). Selective activation of Gαob by an adenosine A. Nat. Commun. *13*, 4150. https://doi.org/10.1038/s41467-022-31652-2.

34. Cueva, J.P., Chemel, B.R., Juncosa, J.I., Lill, M.A., Watts, V.J., and Nichols, D.E. (2012). Analogues of doxanthrine reveal differences between the dopamine D1 receptor binding properties of chromanoisoquinolines and hexahydrobenzo[a]phenanthridines. Eur. J. Med. Chem. *48*, 97–107. https://doi.org/10.1016/j.ejmech.2011.11.039.

35. Harada, K., Ito, M., Wang, X., Tanaka, M., Wongso, D., Konno, A., Hirai, H., Hirase, H., Tsuboi, T., and Kitaguchi, T. (2017). Red fluorescent protein-based cAMP indicator applicable to optogenetics and in vivo imaging. Sci. Rep. *7*, 7351. https://doi.org/10.1038/s41598-017-07820-6.

36. Watts, V.J., Lawler, C.P., Gonzales, A.J., Zhou, Q.Y., Civelli, O., Nichols, D.E., and Mailman, R.B. (1995). Spare receptors and intrinsic activity: studies with D1 dopamine receptor agonists. Synapse *21*, 177–187. https://doi.org/10.1002/syn.890210211.

37. Grimwood, S., and Hartig, P.R. (2009). Target site occupancy: emerging generalizations from clinical and preclinical studies. Pharmacol. Ther. *122*, 281–301. https://doi.org/10.1016/j.pharmthera.2009.03.002.

38. Battaglia, G., Norman, A.B., Hess, E.J., and Creese, I. (1986). Functional recovery of D1 dopamine receptor-mediated stimulation of rat striatal adenylate cyclase activity following irreversible receptor modification by N-ethoxycarbonyl-2-ethoxy-1,2-dihydroquinoline (EEDQ): evidence for spare receptors. Neurosci. Lett. *69*, 290–295. https://doi.org/10.1016/0304-3940(86)90496-9.

39. Reiter, E., Ayoub, M.A., Pellissier, L.P., Landomiel, F., Musnier, A., Tréfier, A., Gandia, J., De Pascali, F., Tahir, S., Yvinec, R., et al. (2017). β-arrestin signalling and bias in hormone-responsive GPCRs. Mol. Cell. Endocrinol. *449*, 28–41. https://doi.org/10.1016/j.mce.2017.01.052.

40. Jean-Charles, P.Y., Kaur, S., and Shenoy, S.K. (2017). G Protein-Coupled Receptor Signaling Through β-Arrestin-Dependent Mechanisms. J. Cardiovasc. Pharmacol. *70*, 142–158. https://doi.org/10.1097/FJC.0000000000000482.

41. Conroy, J.L., Free, R.B., and Sibley, D.R. (2015). Identification of G protein-biased agonists that fail to recruit β-arrestin or promote internalization of the D1 dopamine receptor. ACS Chem. Neurosci. *6*, 681–692. https://doi.org/10.1021/acschemneuro.5b00020.

42. Xiao, P., Yan, W., Gou, L., Zhong, Y.N., Kong, L., Wu, C., Wen, X., Yuan, Y., Cao, S., Qu, C., et al. (2021). Ligand recognition and allosteric regulation of DRD1-Gs signaling complexes. Cell *184*, 943–956.e18. https://doi.org/10.1016/j.cell.2021.01.028.

43. Zhuang, Y., Xu, P., Mao, C., Wang, L., Krumm, B., Zhou, X.E., Huang, S., Liu, H., Cheng, X., Huang, X.P., et al. (2021). Structural insights into the human D1 and D2 dopamine receptor signaling complexes. Cell *184*, 931–942.e18. https://doi.org/10.1016/j.cell.2021.01.027.

44. Teng, X., Chen, S., Nie, Y., Xiao, P., Yu, X., Shao, Z., and Zheng, S. (2022). Ligand recognition and biased agonism of the D1 dopamine receptor. Nat. Commun. *13*, 3186. https://doi.org/10.1038/s41467-022-30929-w.

45. Mabrouk, O.S., Semaan, D.Z., Mikelman, S., Gnegy, M.E., and Kennedy, R.T. (2014). Amphetamine stimulates movement through thalamocortical glutamate release. J. Neurochem. *128*, 152–161. https://doi.org/10.1111/jnc.12378.

46. Wang, J., and O'Donnell, P. (2001). D(1) dopamine receptors potentiate nmda-mediated excitability increase in layer V prefrontal cortical pyramidal neurons. Cereb. Cortex *11*, 452–462. https://doi.org/10.1093/cercor/11.5.452.

47. Chen, G., Greengard, P., and Yan, Z. (2004). Potentiation of NMDA receptor currents by dopamine D1 receptors in prefrontal cortex. Proc. Natl. Acad. Sci. USA *101*, 2596–2600. https://doi.org/10.1073/pnas.0308618100.

48. de Jesús Aceves, J., Rueda-Orozco, P.E., Hernández, R., Plata, V., Ibañez-Sandoval, O., Galarraga, E., and Bargas, J. (2011). Dopaminergic presynaptic modulation of nigral afferents: its role in the generation of recurrent bursting in substantia nigra pars reticulata neurons. Front. Syst. Neurosci. *5*, 6. https://doi.org/10.3389/fnsys.2011.00006.

49. Timmerman, W., and Abercrombie, E.D. (1996). Amphetamine-induced release of dendritic dopamine in substantia nigra pars reticulata: D1-mediated behavioral and electrophysiological effects. Synapse *23*, 280–291. https://doi.org/10.1002/(SICI)1098-2396(199608)23:4<280::AID-SYN6>3.0.CO;2-3.

50. Chuhma, N., Tanaka, K.F., Hen, R., and Rayport, S. (2011). Functional connectome of the striatal medium spiny neuron. J. Neurosci. *31*, 1183–1192. https://doi.org/10.1523/JNEUROSCI.3833-10.2011.

51. Radnikow, G., and Misgeld, U. (1998). Dopamine D1 receptors facilitate GABAA synaptic currents in the rat substantia nigra pars reticulata. J. Neurosci. *18*, 2009–2016.

52. Martin, L.P., and Waszczak, B.L. (1994). D1 agonist-induced excitation of substantia nigra pars reticulata neurons: mediation by D1 receptors on striatonigral terminals via a pertussis toxin-sensitive coupling pathway. J. Neurosci. *14*, 4494–4506.

53. Shirai, F., and Hayashi-Takagi, A. (2017). Optogenetics: Applications in psychiatric research. Psychiatry Clin. Neurosci. *71*, 363–372. https://doi.org/10.1111/pcn.12516.

54. Hervé, D., Lévi-Strauss, M., Marey-Semper, I., Verney, C., Tassin, J.P., Glowinski, J., and Girault, J.A. (1993). G(olf) and Gs in rat basal ganglia: possible involvement of G(olf) in the coupling of dopamine D1 receptor with adenylyl cyclase. J. Neurosci. *13*, 2237–2248.

55. Hubbard, C.A., and Trugman, J.M. (1993). Reversal of reserpine-induced catalepsy by selective D1 and D2 dopamine agonists. Mov. Disord. *8*, 473–478. https://doi.org/10.1002/mds.870080410.

56. Ferré, S., Giménez-Llort, L., Artigas, F., and Martínez, E. (1994). Motor activation in short- and long-term reserpinized mice: role of N-methyl-D-aspartate, dopamine D1 and dopamine D2 receptors. Eur. J. Pharmacol. *255*, 203–213. https://doi.org/10.1016/0014-2999(94)90099-x.

57. Crans, R.A.J., Wouters, E., Valle-León, M., Taura, J., Massari, C.M., Fernández-Dueñas, V., Stove, C.P., and Ciruela, F. (2020). Striatal dopamine D2-muscarinic acetylcholine M1 receptor–receptor interaction in a model of movement disorders. Front. Pharmacol. *11*, 194. https://doi.org/10.3389/fphar.2020.00194.

58. Henry, J.P., Sagné, C., Botton, D., Isambert, M.F., and Gasnier, B. (1998). Molecular pharmacology of the vesicular monoamine transporter. Adv. Pharmacol. *42*, 236–239. https://doi.org/10.1016/s1054-3589(08)60736-x.

59. Morici, J.F., Bekinschtein, P., and Weisstaub, N.V. (2015). Medial prefrontal cortex role in recognition memory in rodents. Behav. Brain Res. *292*, 241–251. https://doi.org/10.1016/j.bbr.2015.06.030.

60. Sun, M., Zhang, Y., Zhang, X.Q., Zhang, Y., Wang, X.D., Li, J.T., Si, T.M., and Su, Y.A. (2024). Dopamine D1 receptor in medial prefrontal cortex mediates the effects of TAAR1 activation on chronic stress-induced cognitive and social deficits. Neuropsychopharmacology *49*, 1341–1351. https://doi.org/10.1038/s41386-024-01866-7.

61. Abi-Dargham, A., Javitch, J.A., Slifstein, M., Anticevic, A., Calkins, M.E., Cho, Y.T., Fonteneau, C., Gil, R., Girgis, R., Gur, R.E., et al. (2022). Dopamine D1R Receptor Stimulation as a Mechanistic Pro-cognitive Target for Schizophrenia. Schizophr. Bull. *48*, 199–210. https://doi.org/10.1093/schbul/sbab095.

62. Mathiasen, J.R., and DiCamillo, A. (2010). Novel object recognition in the rat: a facile assay for cognitive function. Curr. Protoc. Pharmacol. *Chapter 5*, Unit 5.59. https://doi.org/10.1002/0471141755.ph0559s49.

63. Lueptow, L.M. (2017). Novel Object Recognition Test for the Investigation of Learning and Memory in Mice. J. Vis. Exp. *126*, 55718. https://doi.org/10.3791/55718.

64. Antunes, M., and Biala, G. (2012). The novel object recognition memory: neurobiology, test procedure, and its modifications. Cogn. Process. *13*, 93–110. https://doi.org/10.1007/s10339-011-0430-z.

65. Ryman-Rasmussen, J.P., Griffith, A., Oloff, S., Vaidehi, N., Brown, J.T., Goddard, W.A., 3rd, and Mailman, R.B. (2007). Functional selectivity of dopamine D1 receptor agonists in regulating the fate of internalized receptors. Neuropharmacology *52*, 562–575. https://doi.org/10.1016/j.neuropharm.2006.08.028.

66. Floresco, S.B., and Magyar, O. (2006). Mesocortical dopamine modulation of executive functions: beyond working memory. Psychopharmacology (Berl) *188*, 567–585. https://doi.org/10.1007/s00213-006-0404-5.

67. Wenzel, J.M., and Cheer, J.F. (2018). Endocannabinoid Regulation of Reward and Reinforcement through Interaction with Dopamine and Endogenous Opioid Signaling. Neuropsychopharmacology *43*, 103–115. https://doi.org/10.1038/npp.2017.126.

68. Oleson, E.B., Hamilton, L.R., and Gomez, D.M. (2021). Cannabinoid Modulation of Dopamine Release During Motivation, Periodic Reinforcement, Exploratory Behavior, Habit Formation, and Attention. Front. Synaptic Neurosci. *13*, 660218. https://doi.org/10.3389/fnsyn.2021.660218.

69. Ford, C.P., Mark, G.P., and Williams, J.T. (2006). Properties and opioid inhibition of mesolimbic dopamine neurons vary according to target location. J. Neurosci. *26*, 2788–2797. https://doi.org/10.1523/JNEUROSCI.4331-05.2006.

70. Arnsten, A.F.T., Girgis, R.R., Gray, D.L., and Mailman, R.B. (2017). Novel Dopamine Therapeutics for Cognitive Deficits in Schizophrenia. Biol. Psychiatry *81*, 67–77. https://doi.org/10.1016/j.biopsych.2015.12.028.

71. Starr, M.S., and Starr, B.S. (1993). Seizure promotion by D1 agonists does not correlate with other dopaminergic properties. J. Neural Transm. Park. Dis. Dement. Sect. *6*, 27–34. https://doi.org/10.1007/BF02252620.

72. Amenta, F., Ferrante, F., and Ricci, A. (1995). Pharmacological characterisation and autoradiographic localisation of dopamine receptor subtypes in the cardiovascular system and in the kidney. Hypertens. Res. *18*, S23–S27. https://doi.org/10.1291/hypres.18.supplementi_s23.

73. Knoerzer, T.A., Watts, V.J., Nichols, D.E., and Mailman, R.B. (1995). Synthesis and biological evaluation of a series of substituted benzo[a]

phenanthridines as agonists at D1 and D2 dopamine receptors. J. Med. Chem. *38*, 3062–3070. https://doi.org/10.1021/jm00016a009.

74. Stallaert, W., van der Westhuizen, E.T., Schönegge, A.M., Plouffe, B., Hogue, M., Lukashova, V., Inoue, A., Ishida, S., Aoki, J., Le Gouill, C., et al. (2017). Purinergic Receptor Transactivation by the. Mol. Pharmacol. *91*, 533–544. https://doi.org/10.1124/mol.116.106419.

75. Yano, H., Provasi, D., Cai, N.S., Filizola, M., Ferré, S., and Javitch, J.A. (2017). Development of novel biosensors to study receptor-mediated activation of the G-protein α subunits G. J. Biol. Chem. *292*, 19989–19998. https://doi.org/10.1074/jbc.M117.800698.

76. Chan, P., Gabay, M., Wright, F.A., and Tall, G.G. (2011). Ric-8B is a GTP-dependent G protein alphas guanine nucleotide exchange factor. J. Biol. Chem. *286*, 19932–19942. https://doi.org/10.1074/jbc.M110.163675.

77. Vishnivetskiy, S.A., Gimenez, L.E., Francis, D.J., Hanson, S.M., Hubbell, W.L., Klug, C.S., and Gurevich, V.V. (2011). Few residues within an extensive binding interface drive receptor interaction and determine the specificity of arrestin proteins. J. Biol. Chem. *286*, 24288–24299. https://doi.org/10.1074/jbc.M110.213835.

78. Okashah, N., Wan, Q., Ghosh, S., Sandhu, M., Inoue, A., Vaidehi, N., and Lambert, N.A. (2019). Variable G protein determinants of GPCR coupling selectivity. Proc. Natl. Acad. Sci. USA *116*, 12054–12059. https://doi.org/10.1073/pnas.1905993116.

STAR★METHODS

KEY RESOURCES TABLE

REAGENT or RESOURCE	SOURCE	IDENTIFIER
Bacterial and virus strains		
Competent *E. Coli* cells	Takara Bio	Cat# 636763
AAV5-hSyn-hChR2(H134R)-EYFP	Addgene	Addgene Cat# 26973-AAV5
Chemicals, peptides, and recombinant proteins		
Dopamine hydrochloride	Tocris	Cat# 3548
SKF 81297 hydrobromide	Tocris	Cat# 1447
SKF 38393 hydrobromide	Tocris	Cat# 0922
Dihydrexidine hydrochloride	Tocris	Cat# 0844
Methyl-dihydrexidine	Knoerzer et al.[73]	N/A
Doxanthrine	Cueva et al.[34]	N/A
PF-8294	Roche	N/A
PF-6142	Roche	N/A
Tavapadon	Cayman Chemical	Cat# 33556
Reserpine	Tocris	Cat# 2742
Quinpirole hydrochloride	Tocris	Cat# 1061
Experimental models: Cell lines		
Human: 293T	ATCC	Cat# CRL-3216
Human: $G\alpha_{s/olf}$-KO 293T	Stallaert et al.[74]	N/A
Experimental models: Organisms/strains		
Mouse: C57BL/6J	The Jackson Laboratory	RRID: IMSR_JAX:000664
Mouse: B6.Cg-Tg(Drd1a-tdTomato)6Calak/J	The Jackson Laboratory	RRID: IMSR_JAX:016204
Recombinant DNA		
pcDNA3.1-D1R	Yano et al.[75]	N/A
pcDNA3.1-D1R-Rluc8	Yano et al.[75]	N/A
pcDNA3.1-$G\alpha_s$	Yano et al.[75]	N/A
pcDNA3.1-$G\alpha_s$-154Venus	Yano et al.[75]	N/A
pcDNA3.1-$G\alpha_s$-67Venus	Yano et al.[75]	N/A
pcDNA3.1-$G\alpha_{olf}$	Yano et al.[75]	N/A
pcDNA3.1-$G\alpha_{olf}$-155Venus	Yano et al.[75]	N/A
pcDNA3.1-$G\alpha_{olf}$-69Venus	Yano et al.[75]	N/A
pcDNA3.1-$G\alpha_{olf/s}$-ERLAYK	This paper	N/A
pcDNA3.1-β1	Yano et al.[75]	N/A
pcDNA3.1-γ7	Yano et al.[75]	N/A
pcDNA3.1-γ7-Rluc8	Yano et al.[75]	N/A
pcDNA3.1-RIC8B	Chan et al.[76]	N/A
pcDNA3.1-Pink Flamindo	Addgene	Addgene Cat# 102356
pcDNA3.1-β-Arrestin1-Venus	Vishnivetskiy et al.[77]	N/A
pcDNA3.1-β-Arrestin2-Venus	Vishnivetskiy et al.[77]	N/A
pcDNA3.1-GRK2	Vishnivetskiy et al.[77]	N/A
Software and algorithms		
PHERAstar	BMG LABTECH	
Olympus FV31S-SW	Olympus	
HC Image Live	Hamamatsu	
pClamp 11	Molecular Devices	

(*Continued on next page*)

Continued

REAGENT or RESOURCE	SOURCE	IDENTIFIER
Doric Neuroscience Studio	Doric Lenses	
PyMOL 3.1.1	Schrodinger	
Activity Monitor 7.8.0.0	MED Associates	
ANY-maze 7.4	Stoelting Co.	
GraphPad Prism 10	GraphPad Software	
Office 365	Microsoft	
Adobe Illustrator	Adobe	

EXPERIMENTAL MODEL AND STUDY PARTICIPANT DETAILS

Cell lines

HEK293T (ATCC Cat# CRL-3216) and $G\alpha_{s/olf}$-KO 293A cells were cultured in Dulbecco's modified Eagle's medium (DMEM) containing 10% fetal bovine serum (FBS), 2 mM L-glutamine and 1% penicillin-streptomycin at 37°C and incubated in 5% CO2 – 95% moisturized air.

Mouse strains

All experiments were conducted under the guidelines provided by the Institutional Animal Care and Use Committee at Northeastern University (protocol number 22-1031R), per applicable laws and regulations. Wildtype (C57BL/6J, RRID: IMSR_JAX:000664) and Drd1a-tdTomato (B6.Cg-Tg(Drd1a-tdTomato)6Calak/J, RRID: IMSR_JAX:016204) mice were maintained on a 12-h light/dark cycle with food and water supply *ad libitum*. Mice aged 12 to 20 weeks old were used for the experiments, and littermates of both sexes were randomly assigned to each experiment group. All mice were drug-naïve before the experiments.

METHOD DETAILS

Transfection

HEK293T or CL4 cells were seeded at 4 million cells per 10-cm plate. A constant amount of cDNA was transfected using polyethyleneimine (PEI) (1:2 w/w). For engagement BRET assays, CL4 cells were transfected with D1R-RLuc8 (Renilla Luciferase), $G\alpha_s$-154Venus or $G\alpha_{olf}$-155Venus, Gβ2, Gγ7, and RIC8B. For activation BRET assays, CL4 cells were transfected with untagged D1R, $G\alpha_s$-67Venus or $G\alpha_{olf}$-69Venus, Gβ2, Gγ7-RLuc8, and RIC8B. For cAMP production assays, CL4 cells were transfected with D1R, $G\alpha_s$ or $G\alpha_{olf}$ or $G\alpha_{olf}\alpha$N, Gβ2, Gγ7, RIC8B, and Pink Flamindo (a fluorescence-based cAMP biosensor). For β-Arrestin recruitment assays, WT cells were transfected with D1R-RLuc8, β-arrestin1-Venus or β-arrestin2-Venus, and GRK2. The ratio between the transfected constructs had been previously optimized for the dynamic range of the drug-induced BRET change, as described previously.[30]

Bioluminescence resonance energy transfer (BRET)

Forty-eight hours post-transfection, cells were harvested and resuspended in potassium-based buffer (140 mM KCl, 10 mM NaCl, 1 mM $MgCl_2$, 0.1 mM KEGTA, 20 mM NaHEPES, pH 7.2) for engagement and activation BRET or phosphate-buffered saline (PBS) containing 200 μM sodium bisulfite (NaBi) for β-Arrestin recruitment assays. Cells were distributed at 100,000 cells per well in a white 96-well plate and 5 μM coelenterazine H was added. Ligands at varying concentrations were added 1 minute later. For engagement and activation BRET assays with $G\alpha_{olf}$, cells were pre-incubated with 10 μg/ml digitonin for 60 minutes prior to ligand addition.[78] Bioluminescence and fluorescence emissions were recorded at 485 and 530 nm, respectively.

cAMP production assay using the biosensor Pink Flamindo

Cells were prepared as described above for the BRET assay, except that they were resuspended in PBS containing 200 μM Na Bisulfite and distributed in a black 96-well plate. The plate reader is set at 540 nm excitation and 590 nm emission. For the experiments with EEDQ, cells were treated with 100 μM EEDQ at room temperature for 1 h before the D1R agonists were introduced.

Stereotaxic surgery

Drd1a-tdTomato BAC transgenic mice were anesthetized and maintained with isoflurane/oxygen through a nose cone mounted on a stereotaxic apparatus. The scalp was opened, and two holes were drilled in the skull (-0.4 mm AP, ±0.4 mm ML, -3.5 mm DV from bregma for the thalamocortical pathway; 0 mm AP, ±2 mm ML, -3 mm DV from bregma for the nigrostriatal pathway). AP, ML, and DV, which stand for anterior-posterior, medial-lateral, and dorsal-ventral, respectively, were the spatial coordinates relative to the

bregma. AAV5-hSynapsin-hChannelrhodopsin 2(H134R)-EYFP virus at a titer of 2 x 10^{13} vg/ml (0.5 μl/side) was injected at 0.1 μl/min. The needle was left in place for 1 minute before being slowly removed.

Slice electrophysiology

Horizontal (for the nigrostriatal pathway) and coronal slices (for the thalamocortical pathway) at 220 μm thickness were prepared using a vibratome (VT-1000S, Leica) to capture the substantial nigra reticulata (bregma -4.90 - -3.75 mm) and prelimbic/infralimbic parts of the medial prefrontal cortex (bregma 1.20 - 1.95 mm). Mice were anesthetized with isoflurane and perfused with modified artificial cerebral spinal fluid (m-aCSF) containing (in mM): 92 NMDG, 20 HEPES, 25 glucose, 30 $NaHCO_3$, 1.2 NaH_2PO_4, 2.5 KCl, 5 sodium ascorbate, 3 sodium pyruvate, 2 thiourea, 10 $MgSO_4$, 0.5 $CaCl_2$, 300–310 mOsm, and pH 7.3–7.4. Slices were sectioned in cold m-aCSF, recovered at 32 °C in the same buffer saturated with carbogen for 10 min, and transferred to a holding chamber filled with carbogen-saturated aCSF (holding aCSF) containing (in mM): 92 NaCl, 20 HEPES, 25 glucose, 30 $NaHCO_3$, 1.2 NaH_2PO_4, 2.5 KCl, 5 sodium ascorbate, 3 sodium pyruvate, 2 thiourea, 1 $MgSO_4$, 2 $CaCl_2$, 300–310 mOsm, and pH 7.3–7.4. During recordings, slices were continuously perfused at 2 ml/min with carbogen-saturated aCSF containing (in mM): 124 NaCl, 2.5 KCl, 1.25 NaH_2PO_4, 1 $MgCl_2$, 26 $NaHCO_3$, 11 glucose, 2.4 $CaCl_2$, 300–310 mOsm, and pH 7.3–7.4. The temperature of the recording chamber was maintained at 31–32°C. Electrodes (3–5 MΩ) were backfilled with an internal solution containing (in mM): 120 mM K gluconate, 20 KCl, 0.05 EGTA, 10 HEPES, 1.5 $MgCl_2$, 2.18 Na_2 ATP, 0.38 Na GTP, 10.19 Na phosphocreatine, 280–285 mOsm, and pH 7.3–7.4. Pyramidal neurons in layer V of the mPFC and GABAergic neurons in the SNr were visually identified using IR-DIC optics with an upright microscope (Olympus). Whole-cell voltage-clamp recordings (held at resting membrane potential) were made using a MultiClamp 700B amplifier (2 kHz low-pass Bessel filter and 10 kHz digitization) with pClamp 11 software (Molecular Devices).

For ChR2 evoked responses, the thalamocortical and striatonigral terminals were photostimulated using a 473 nm DPSS blue laser. The laser was controlled by an Optogenetics TTL Pulse Generator (Doric Lenses, Quebec, Canada). The stimulation protocol consisted of 4 pulsed lights at 5 s intervals with a 2 ms pulse duration at 1 mW, followed by a 40 s pause. After voltage-clamp recording was established, cell response to photostimulation in the absence of the drugs (baseline) was recorded for 20 minutes followed by 6 – 10 minutes of drug perfusion at the rate of 1 – 2 ml/min. Peak amplitudes in the last 3 minutes of each condition were used for statistical analysis.

For the thalamocortical pathway, the following numbers of slices were recorded for each drug condition: 1 μM SKF 81297 (15 recordings from 7 animals), 1 μM SKF 81297 and 10 μM SCH 23390 (10 recordings from 4 animals), 1 μM DHX (9 recordings from 5 animals), 1 μM TAV (8 recordings from 6 animals). For the nigrostriatal pathway, the following numbers of slices were recorded for each drug condition: 1 μM SKF 81297 (8 recordings from 4 animals), 1 μM SKF 81297 and 10 μM SCH 23390 (7 recordings from 4 animals), 1 μM DHX (6 recordings from 5 animals), 1 μM TAV (7 recordings from 5 animals).

Locomotor assay

Reserpine 3 mg/kg (injection volume 10 μl/g bodyweight) was administered subcutaneously 18 – 20 h before undertaking the behavioral assays. Following the 18 – 20 h period, mice were injected intra-peritoneally with a cocktail of quinpirole 1 mg/kg and either SKF 81297, DHX, or TAV at 1, 3, 6 mg/kg (injection volume 10 μl/g bodyweight). Mice were introduced to a 28 cm x 28 cm open-field arena (ENV-520, Med Associate Inc.) for a 60-minute recording session in 4 bins of 15 minutes. Data was reported as the average ambulatory distance (cm) in 1 bin.

Novel object recognition assay

Each mouse was handled for at least 2 minutes every day for one week before it was habituated to an empty arena (43 cm x 43 cm) for 5 minutes the day before the familiarization phase. In the familiarization phase, mice were allowed to freely explore the arena with 2 identical objects placed diagonally for 7 minutes. Then, they were returned to their home cage for an inter-trial interval (ITI) of 24 h. On the test day, mice were injected with saline, SKF 81297, DHX or TAV at 6 mg/kg (injection volume 10 μl/g bodyweight) 60 minutes before the trial. During the testing trial, mice were allowed to explore the arena with 2 objects placed diagonally, 1 from the familiarization phase and 1 novel object for 7 minutes. The objects used in the familiarization phase were randomly chosen, and the positions of the familiar and the novel objects were randomly assigned for each test animal to minimize the effects of object and place preference. Exploratory behavior was defined as the mice having their nose pointed toward the objects and the distance between the nose and the object was less than 2 cm. All phases of the assay were recorded on video, and the time spent exploring each object was determined using ANY-maze. If any mice failed to reach a total of 14 s of exploration time in either the familiarization or testing phase, they would be excluded from data analysis. Data was reported as discriminatory index (DI), which was calculated using the following equation:

$$DI = \frac{time\ exploring\ new\ object - time\ exploring\ familiar\ object}{total\ exploring\ time}$$

QUANTIFICATION AND STATISTICAL ANALYSIS

All experiments were conducted independently at least 5 times. For *in vitro* assays, the value of n represents the number of independent experiments. For electrophysiology experiments, the value of n represents the number of recordings. For the behavioral assay, the value of n represents the number of animals. Data is shown as mean ± S.E.M (standard error of the mean) with or without individual data points. Statistical details, including statistical tests and defined confidence intervals based on p-values of the experiments, are described in the figure legends. Statistical comparisons were made using GraphPad Prism 10. One-way ANOVA followed by the recommended post-hoc analysis by Prism was used to make comparisons between conditions.